Supporting Information

Detecting Labile Heme and Ferroptosis Through 'Turn-On' Fluorescence and lipid droplet localization post Fe2+ sensing

Yogesh Dubey[#], Shabnam Mansuri[#] and Sriram Kanvah*

[*]Department of Chemistry, Indian Institute of Technology Gandhinagar, Palaj, Gandhinagar, Gujarat – 382055: Email: sriram@iitgn.ac.in

#Equal Authorship

Table of Contents

S1. Synthetic procedure

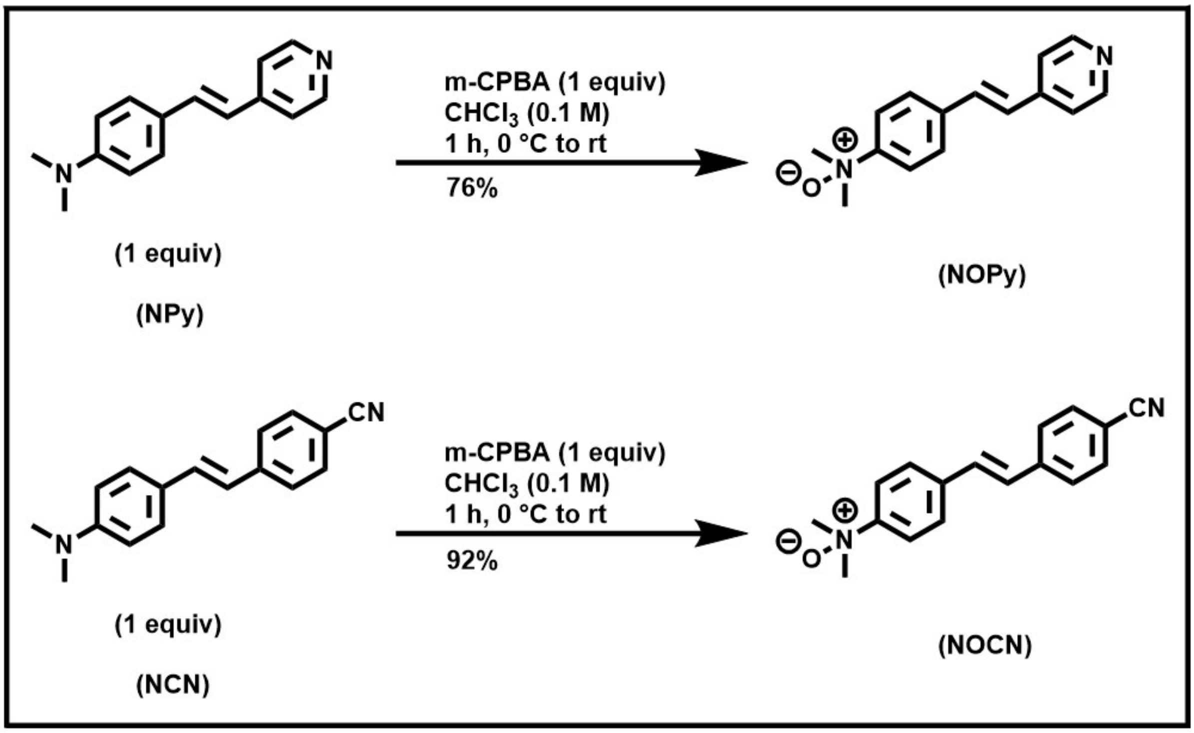

General procedure: NPy/NCN (1 equiv) in chloroform (0.1M) was placed in a round-bottomed flask, and m-CPBA (1 equiv) was added in small portions with the temperature maintained at 0 °C. The reaction mixture was gradually brought to room temperature and stirred for 1 hour until all the starting material was consumed, as monitored on a chromatographic TLC plate. Upon completion of the reaction, chloroform was evaporated using a rotary evaporator, and the residue was directly loaded onto a basic alumina oxide stationary phase, isolated, and weighed"

For NOPy, TLC system – 10 % methanol in DCM – Rf (0.45). Column eluent – 1 to 8 % gradient elution of methanol in DCM;

For NOCN, TLC system – 5 % methanol in Dichloromethane – Rf (0.30); Column eluent – 1 to 8 % gradient elution of methanol in Dichloromethane.

The compounds NPy and NCN were synthesized from the literature procedure[1,2].

Figure S2. Response to Fe^{2+} by NOPy

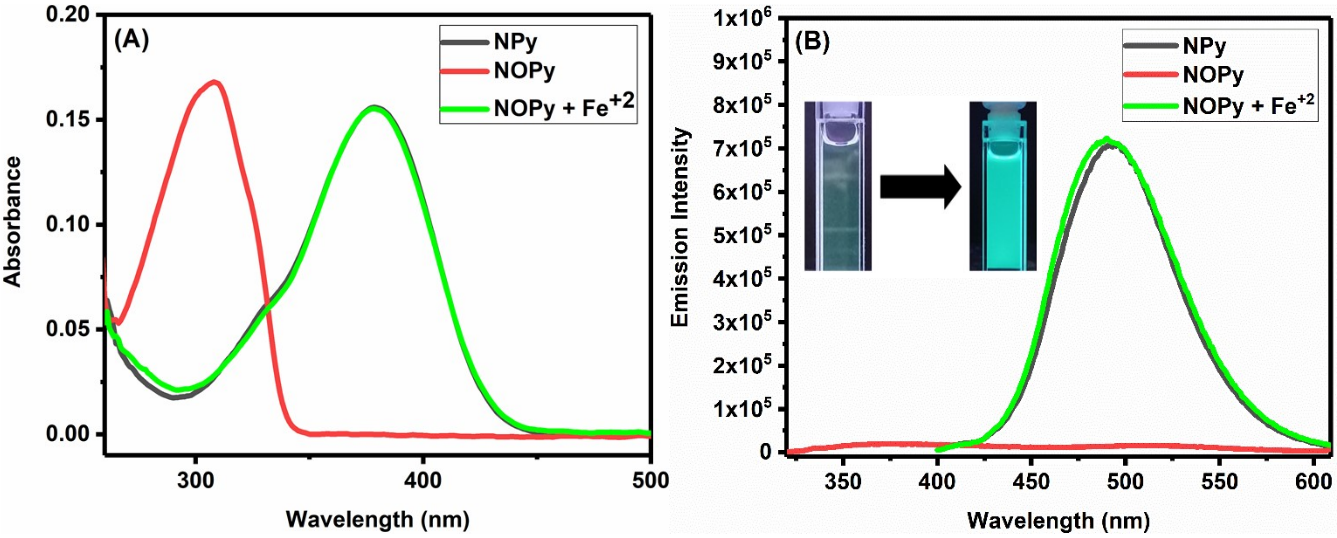

Fig. S2 Comparative (A) Absorption spectra of NPy, NOPy, NOPy with Fe^{+2} and (B) Emission spectra for NPy, NOPy, NOPy with Fe^{2+} in DMSO [20 µM of dye (in DMSO) and 20 µM of Fe^{2+} (in water)]

Figure S3. Absorption and emission titration with varying concentration of Fe^{2+} for NOPy (20µM)

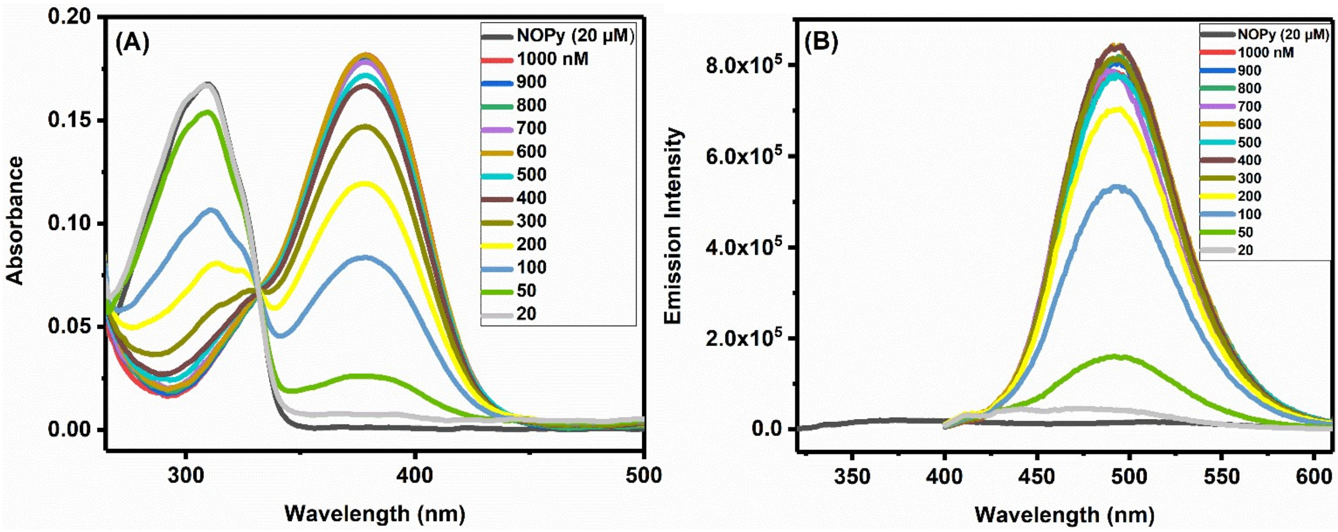

Fig. S3 (A) Absorption titration with varying concentration of Fe^{2+} in DMSO (B) Emission titration with varying concentration of Fe^{2+}

Figure S4. Limit of detection

The detection limit of the probe can be calculated using the formula - LOD = (3 x R^2)/m, where R^2 is R-square and m is the slope of the $F_/F_0$ versus Fe^{2+} concentration. To get the slope, the $F_/F_0$ at 490 nm and 536 nm for NOPy and NOCN, respectively, was plotted against a concentration of Fe^{2+}.

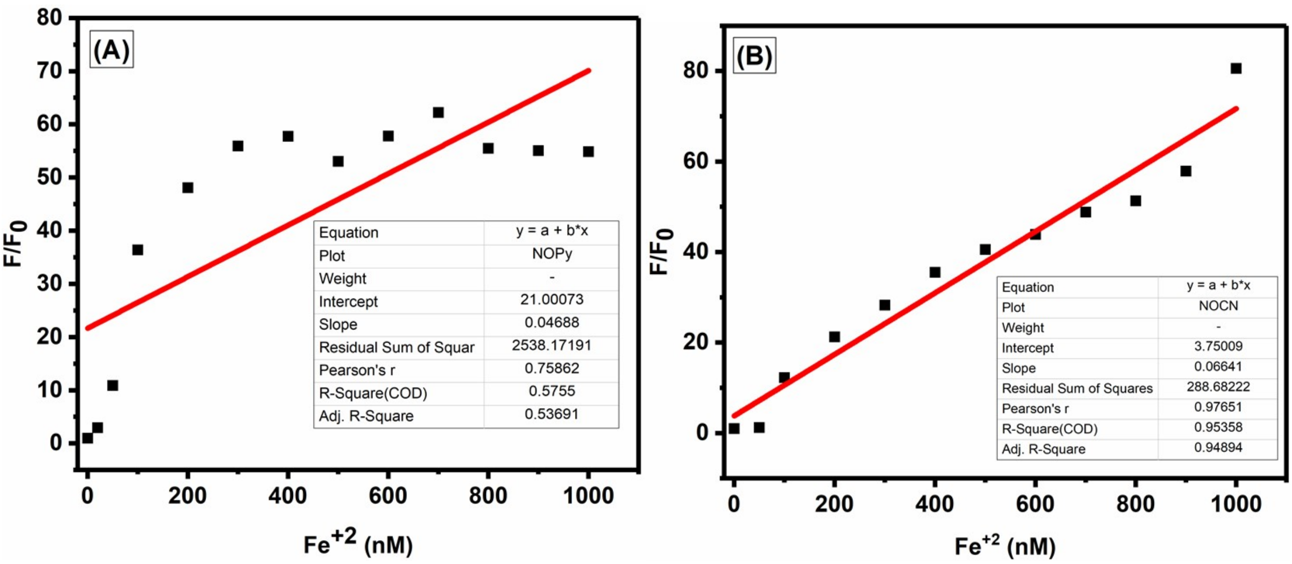

Fig. S4 LOD plot for (A) NOPy and (B) NOCN

Table S5. Comparison of NOPy and NOCN with several recently reported N-oxide probes for the detection of Fe^{2+}

Probe	Time (min)	LOD (µM)	Reference
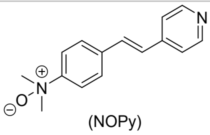 (NOPy) 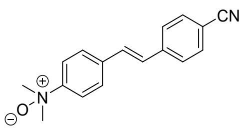 (NOCN)	Instant (~0.16)	**NOPy**- 0.035 **NOCN**-0.042	This work
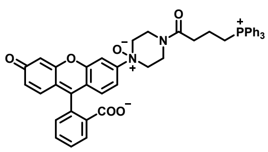	30	0.81	Metallomics, 2018, 10(6), 794-801

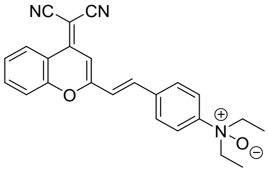	15	4.5	Sensors Actuators B: Chem., 2019, 288, 217-224.
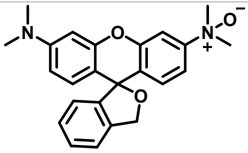	20	0.2	Org. Biomolecular Chem. 2014, 12(34), 6590-6597
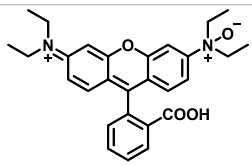	-	0.2	Chemical science, 2013, 4(3), 1250-1256
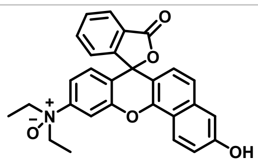	5	0.15	Sensors Actuators B: Chem. 2020, 305, 127470.
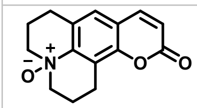	30	-	Chem. Science, 2017, 8(7), 4858-4866
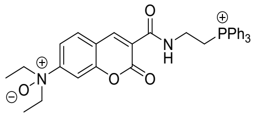	30	1.03	J. Photochem. Photobiol.B: Biol., 2020, 209, 111943
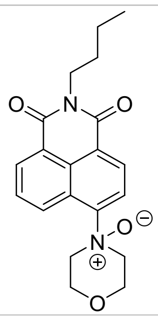	60	1.02	Chemical Communications, 2019, 55(81), 12136-12139.

Figure S6. Selectivity and strip test of NOCN

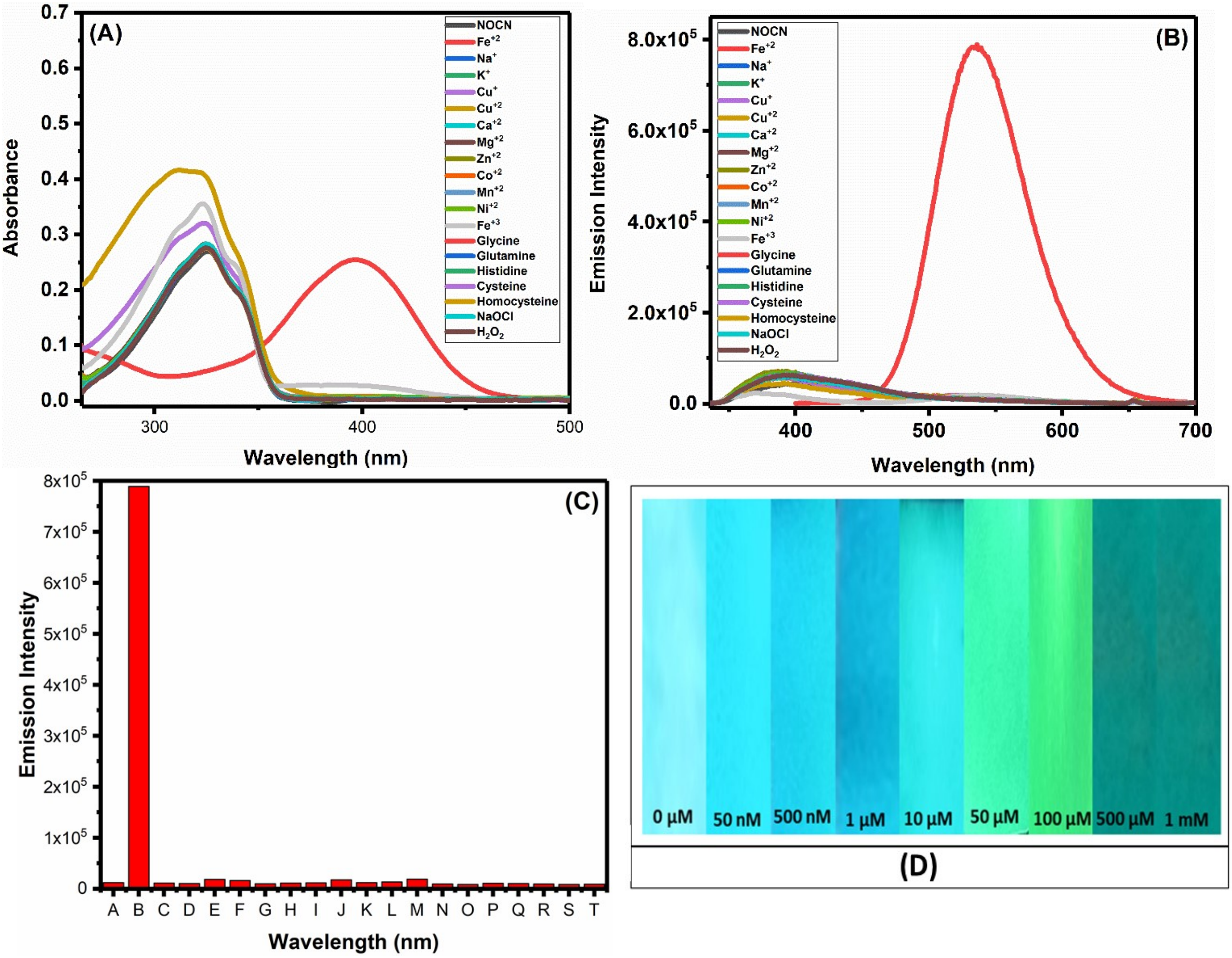

Fig. S6 20 μM probe titration against various 20 μM of analyte supplemented as their chloride salt (A) Absorption and (B) emission spectra for NOCN with different analytes in DMSO (C) Emission intensity changes for NOPy with Fe(II) compared with analytes [A to T = None, Fe^{2+}, Na^{+}, K^{+}, Cu^{+}, Cu^{2+}, Ca^{2+}, Mg^{2+}, Zn^{2+}, Co^{2+}, Mn^{2+}, Ni^{2+}, Fe^{3+}, Glycine, Glutamine, Histidine, Cysteine, Homocysteine, NaOCl, H_2O_2 and (D) color variations as obtained through chromatographic strip paper (NOCN) in water (Fe^{2+} conc. mentioned on strip paper).

.

Figure S7. Comparative NMR spectra for NPy[2] vs DNO[3] vs NOPy

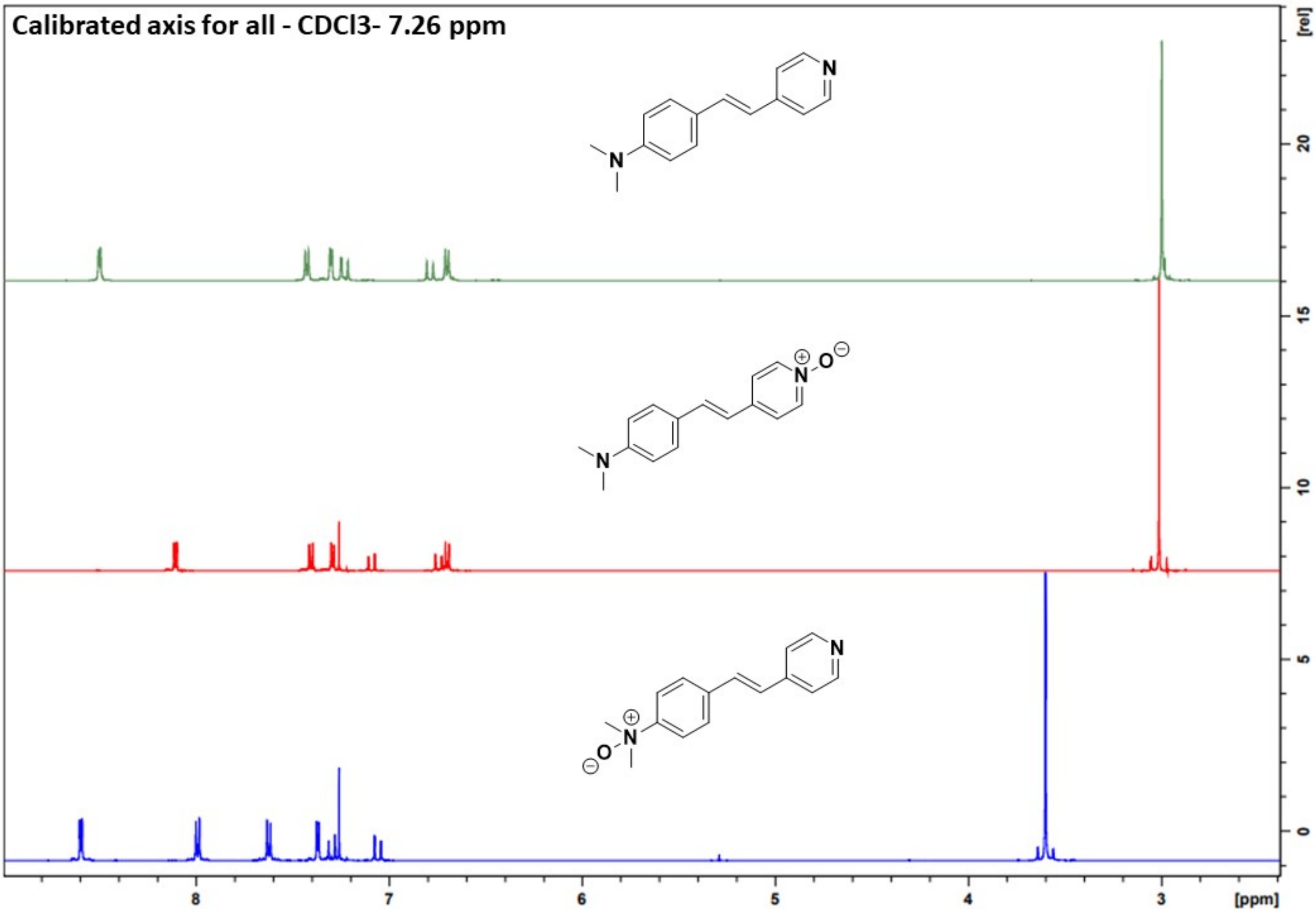

Figure S8. Cytotoxicity assay for NOPy and NOCN at various concentrations.

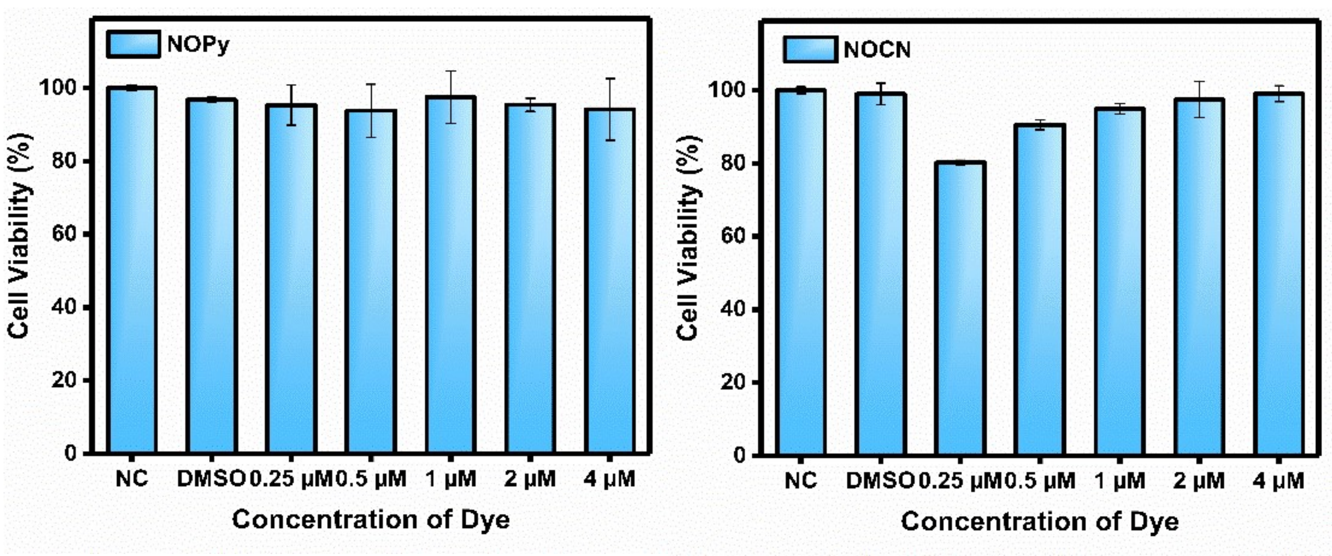

Figure S9. Solubility test

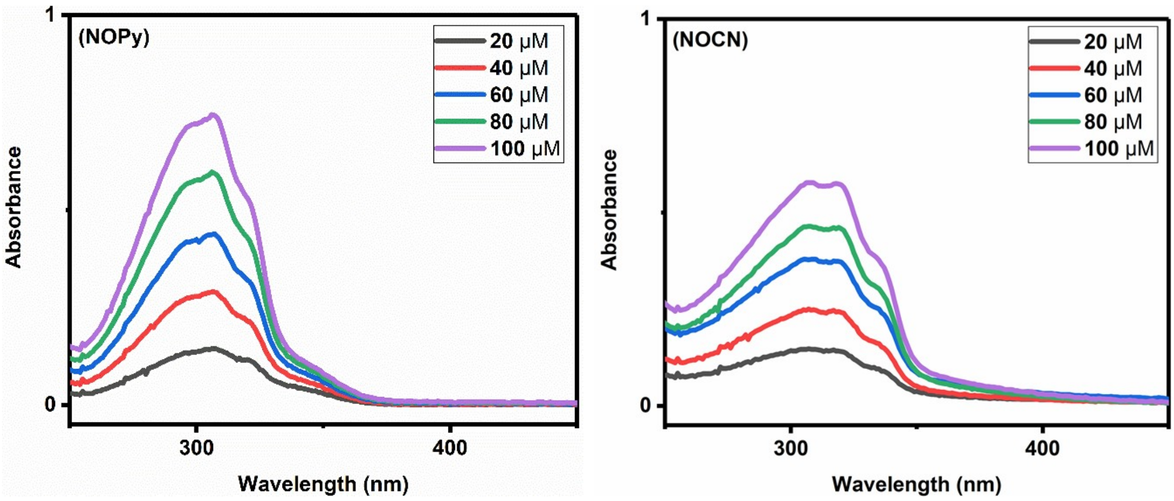

Fig S9A. Uv-Vis plot for NOPy (left panel) and NOCN (right panel) with increasing concentration of probe in water

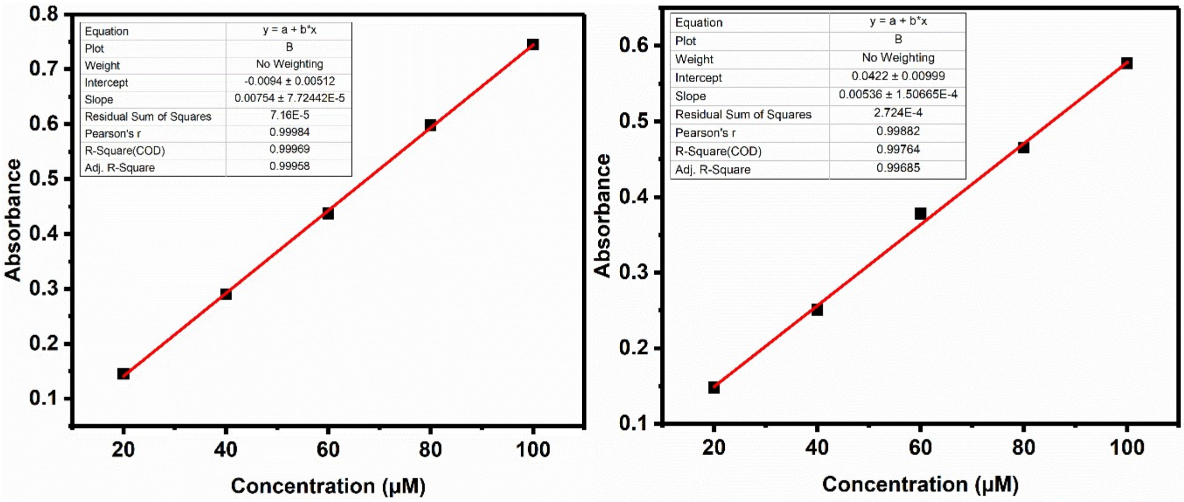

Fig S9B. Uv-Vis calibration curve plot for NOPy (left panel) and NOCN (right panel)

Figure S10. Response to pH

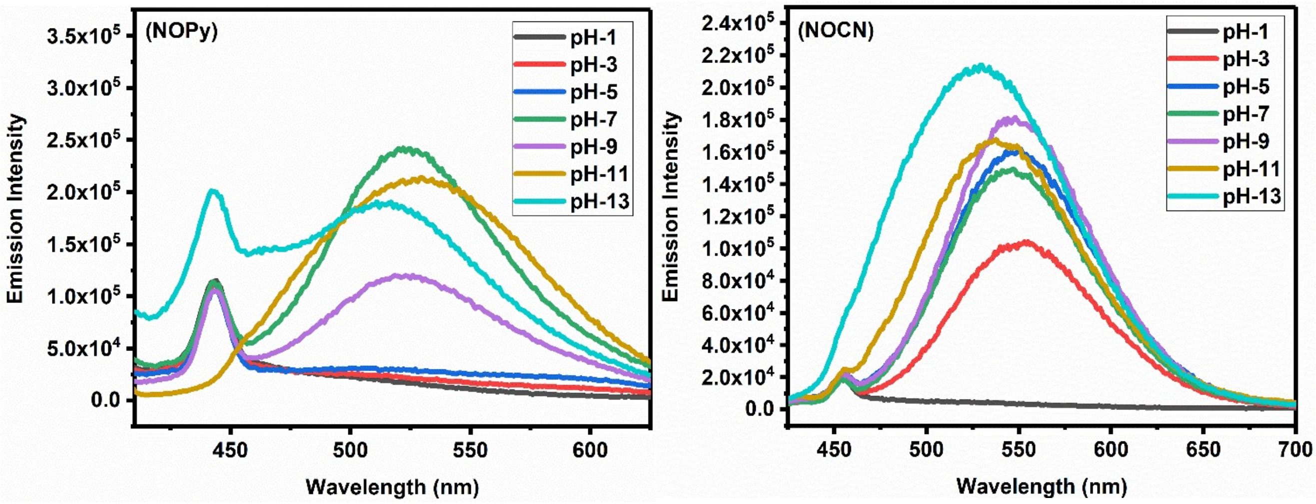

Fig. S10 pH response of NOPy and NOCN at various pH

[20 μM of dye (in DMSO) + 20 μM of Fe(II) (in water)] is taken in water of pH-1,3,5,7,9,11,13.

S11. Characterization Data

1. (E)-N,N-dimethyl-4-(2-(pyridin-4-yl)vinyl)aniline oxide (NOPy)

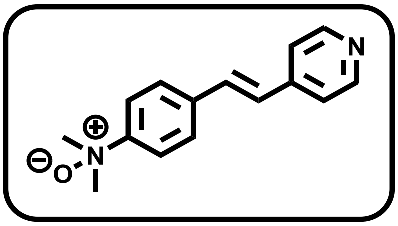

^{1}H NMR (500 MHz, $CDCl_3$): δ 8.61 (d, J = 5.0 Hz, 2H), 8.02 (d, J = 5.0 Hz, 2H), 7.64 (d, J = 5.0 Hz, 2H), 7.38 (d, J = 5.0 Hz, 2H), 7.31 (d, J = 15 Hz , 1H), 7.07 (d, J= 16.5 Hz, 1H), 3.61 (s, 6H). **^{13}C NMR** (126 MHz; $CDCl_3$) δ 154.39, 150.19, 143.89, 136.78, 131.19, 127.72, 127.46, 120.85, 120.53, 63.38. **HRMS** (ESI) m/z calcd for $C_{15}H_{17}N_2O^+$ $[M + H]^+$ 241.1335, found 241.1317. IR in $CHCl_3$ (cm^{-1}) : 3020, 1595, 1503, 1459, 1418, 1214, 967, 835, 744, 667, 571. Melting point : 145-148 °C.

2. (E)-4-(4-cyanostyryl)-N,N-dimethylaniline oxide (NOCN)

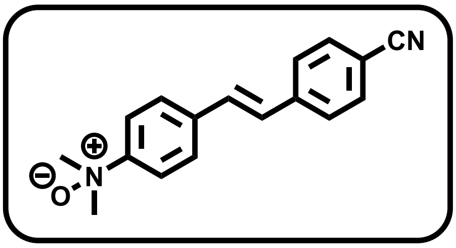

^{1}H NMR (500 MHz, $CDCl_3$): δ 7.94 (d, J = 8.5 Hz, 2H), 7.55 (m, 6H), 7.15 (d, J = 16.0 Hz, 1H), 7.06 (d, J = 16.0 Hz, 1H), 3.54 (s, 6H). **^{13}C NMR** (126 MHz; $CDCl_3$) δ 153.31, 140.20, 136.04, 131.53, 129.48, 127.52, 126.43, 126.05, 119.60, 117.87, 110.04, 62.42. **HRMS** (ESI) m/z calcd for $C_{17}H_{18}N_2O^+$ $[M + H]^+$ 265.1335, found 265.1355. IR in $CHCl_3$ (cm^{-1}): 3272, 2957, 2920, 2848, 2224, 1601, 1507, 1460, 1417, 1203, 969, 841, 770, 571. Melting point : 171-173 °C.

1. (E)-N,N-dimethyl-4-(2-(pyridin-4-yl)vinyl)aniline oxide (NOPy)

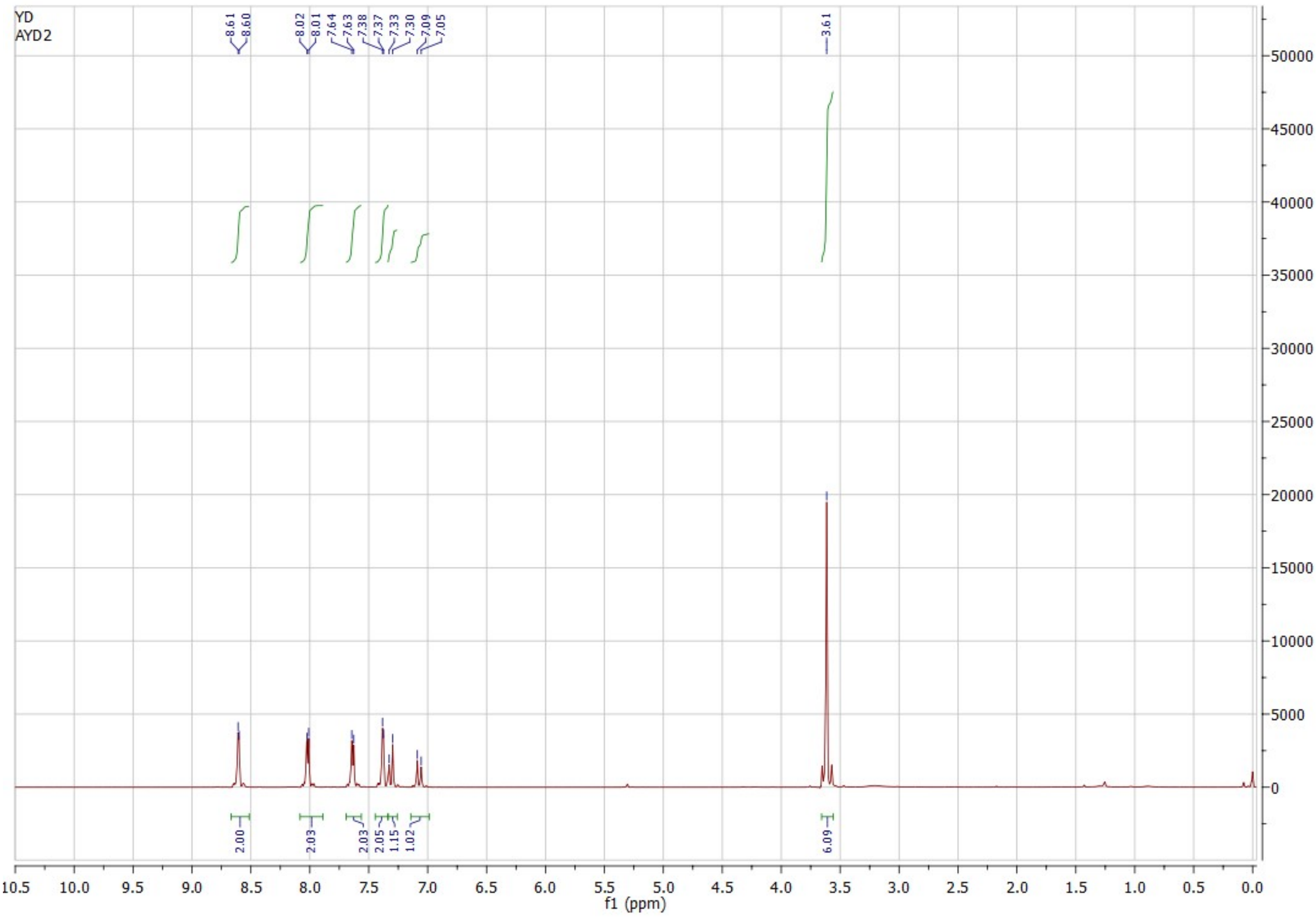

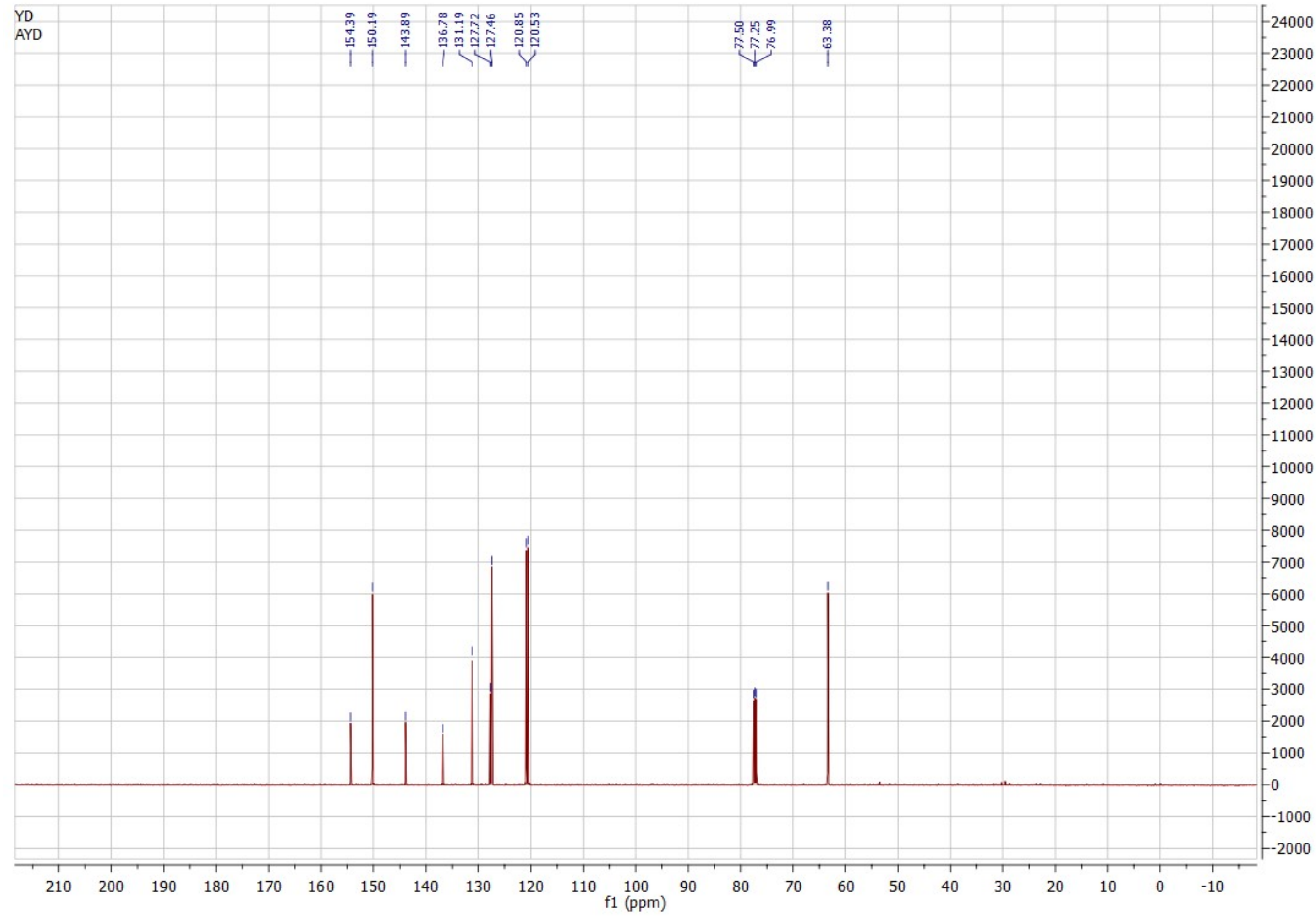

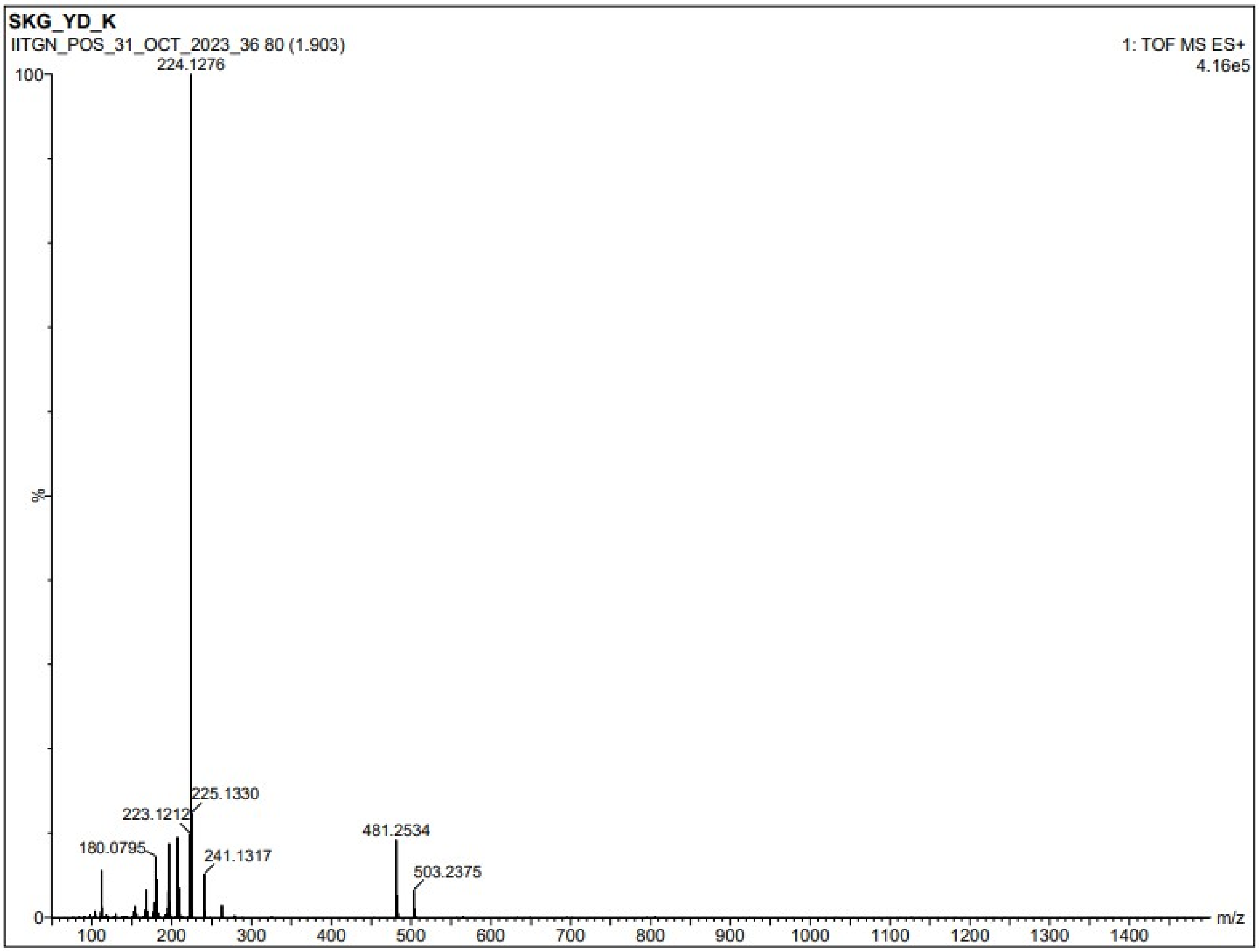
SKG_YD_K
IITGN_POS_31_OCT_2023_36 80 (1.903)
1: TOF MS ES+
4.16e5
224.1276
225.1330
223.1212
180.0795
241.1317
481.2534
503.2375
%
m/z

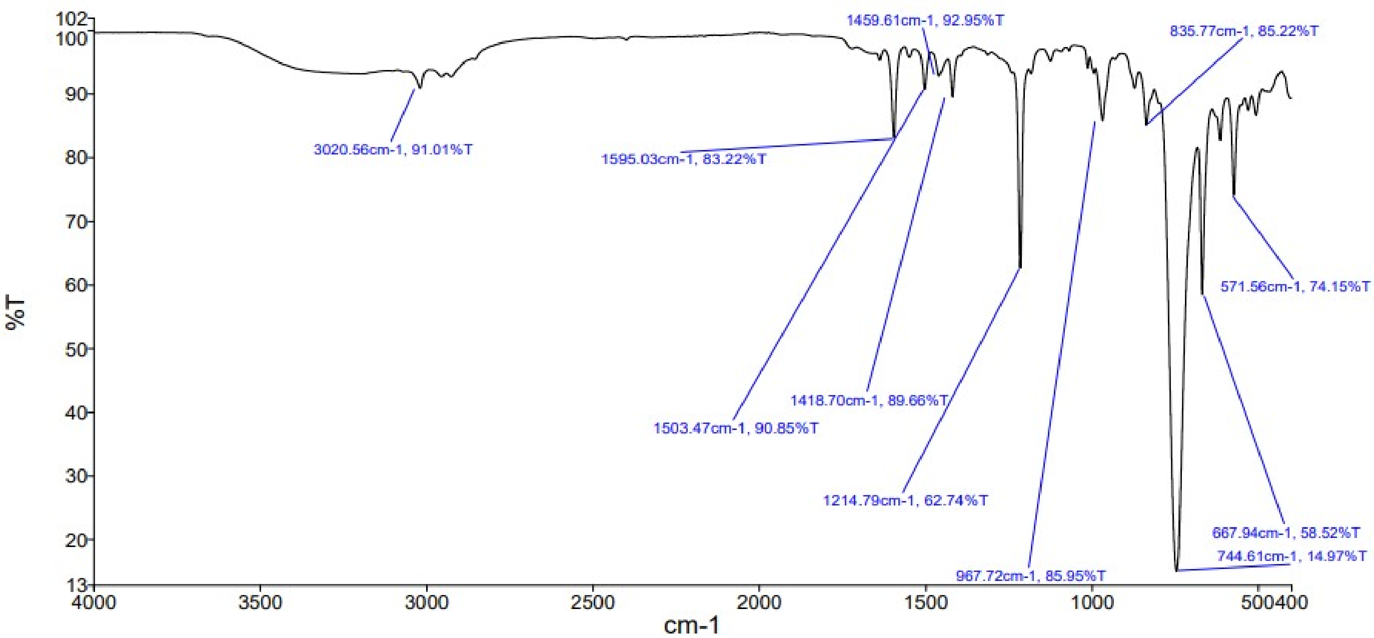
1459.61cm-1, 92.95%T
835.77cm-1, 85.22%T
3020.56cm-1, 91.01%T
1595.03cm-1, 83.22%T
571.56cm-1, 74.15%T
1418.70cm-1, 89.66%T
1503.47cm-1, 90.85%T
1214.79cm-1, 62.74%T
667.94cm-1, 58.52%T
744.61cm-1, 14.97%T
967.72cm-1, 85.95%T
%T
cm-1

2. (E)-4-(4-cyanostyryl)-N,N-dimethylaniline oxide (NOCN)

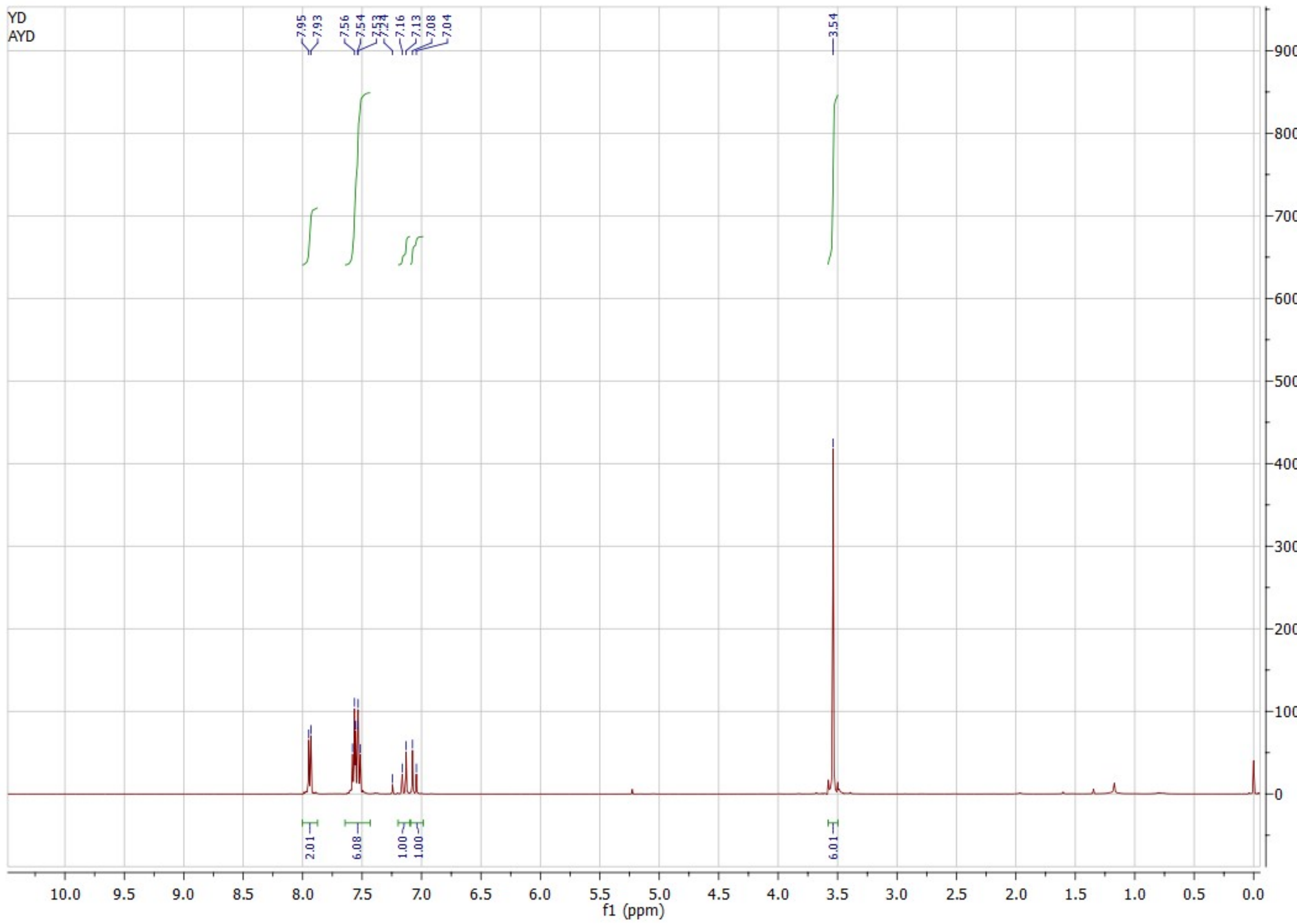

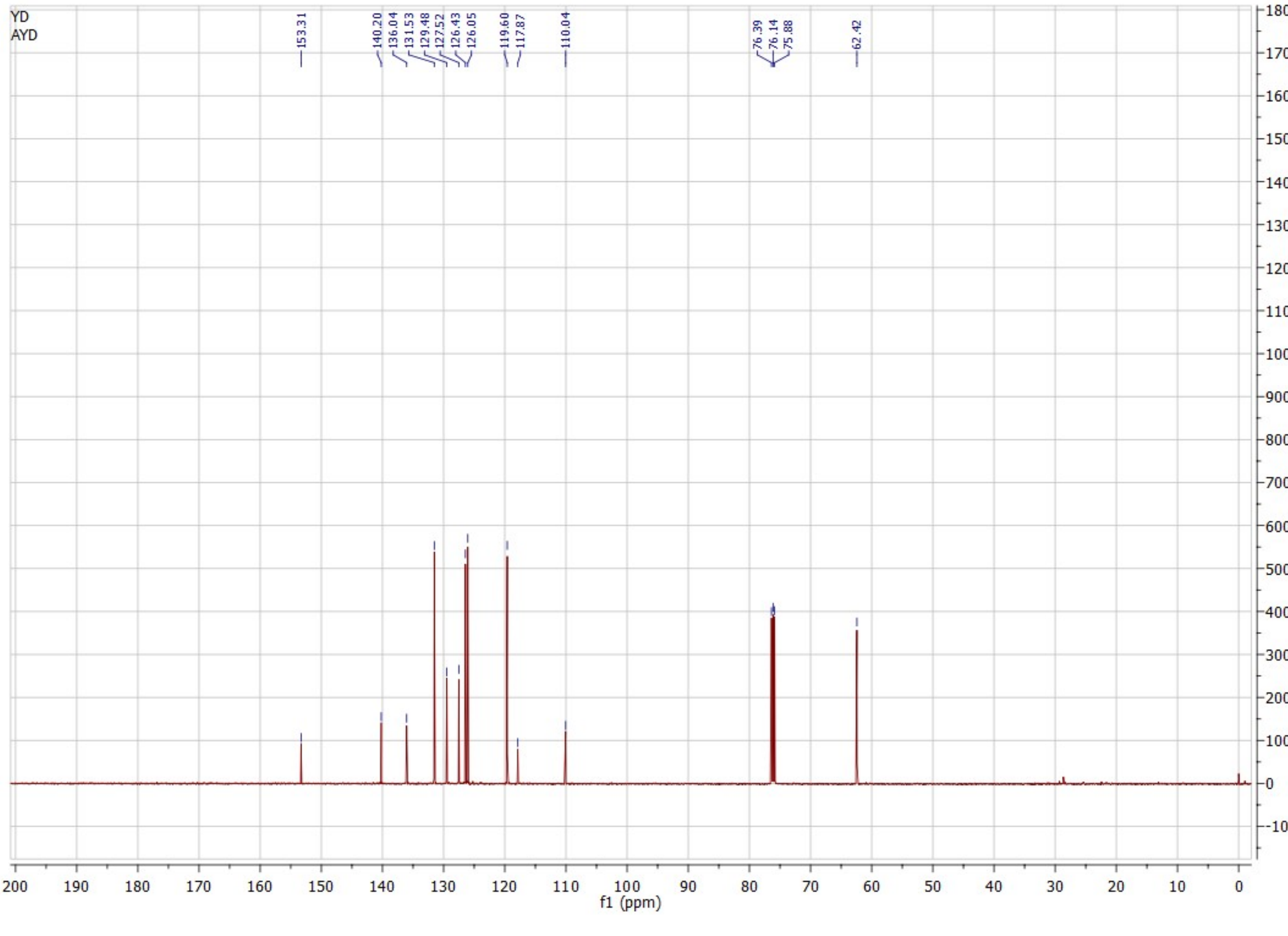

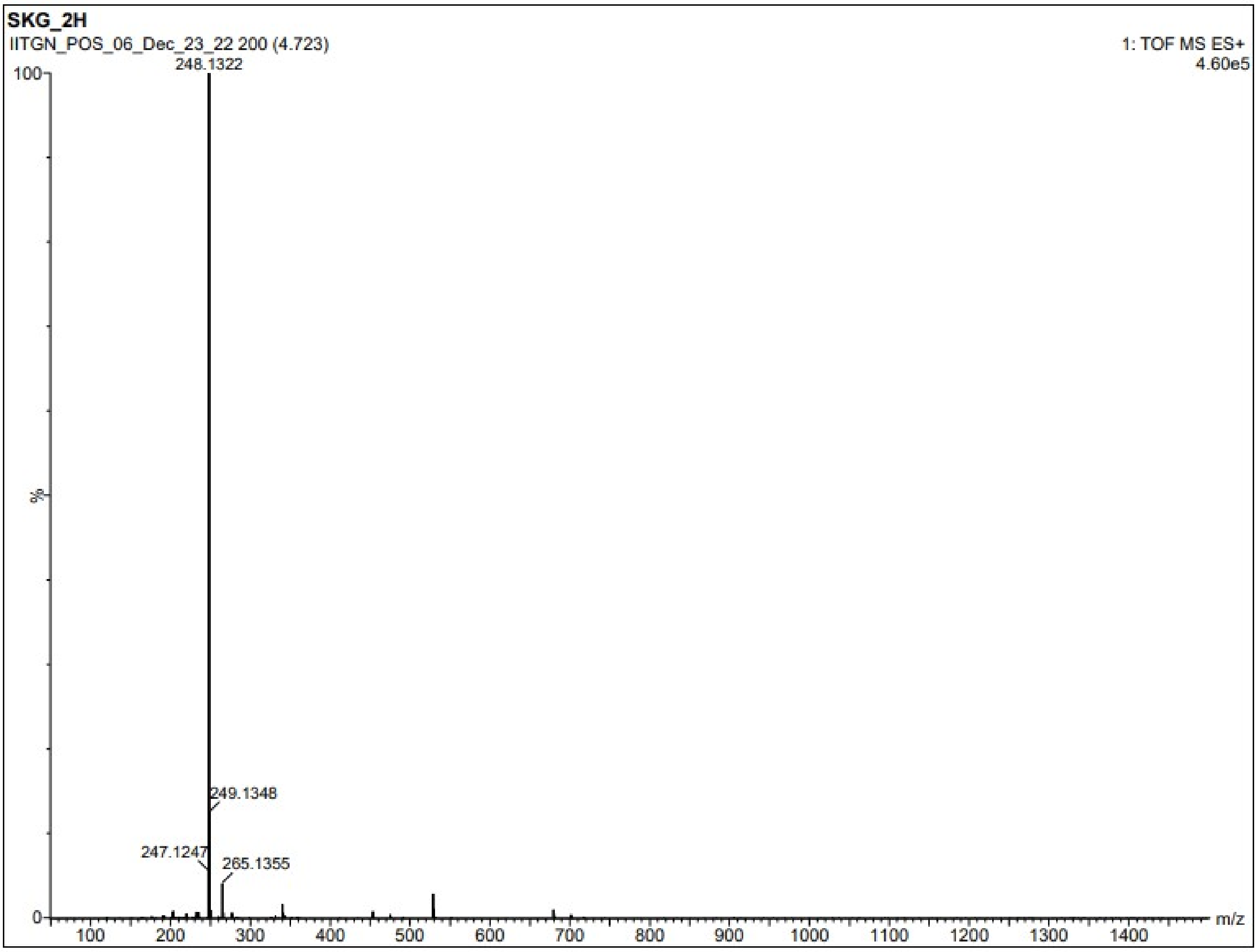

SKG_2H
IITGN_POS_06_Dec_23_22 200 (4.723)
1: TOF MS ES+
4.60e5
248.1322
249.1348
247.1247
265.1355
%
m/z

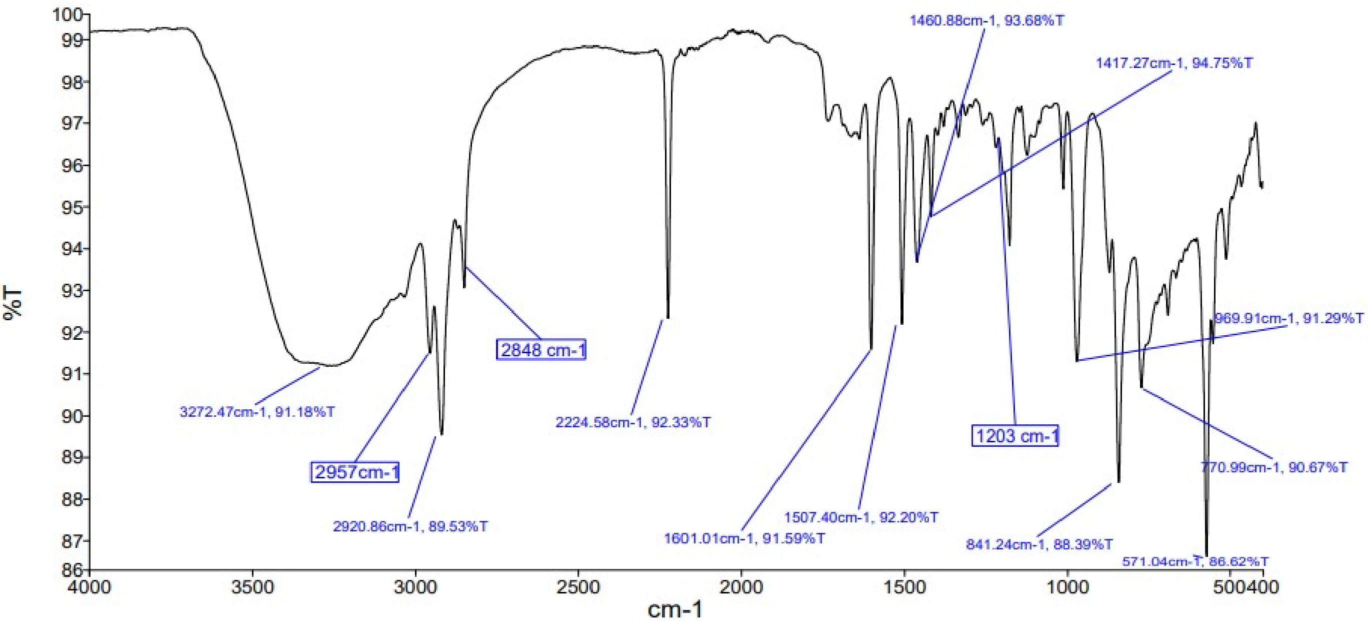

1460.88cm-1, 93.68%T
1417.27cm-1, 94.75%T
2848 cm-1
969.91cm-1, 91.29%T
3272.47cm-1, 91.18%T
2957cm-1
2224.58cm-1, 92.33%T
1203 cm-1
2920.86cm-1, 89.53%T
1601.01cm-1, 91.59%T
1507.40cm-1, 92.20%T
841.24cm-1, 88.39%T
770.99cm-1, 90.67%T
571.04cm-1, 86.62%T
%T
cm-1

S12. References

1. Cariati, E., Cavallo, G., Forni, A., Leem, G., Metrangolo, P., Meyer, F., Pilati, T., Resnati, G., Righetto, S., Terraneo, G. and Tordin, E., *Crystal growth & design*, 2011, *11*(12), 5642-5648.
2. Mukherjee, T., Siva, M. A., Bajaj, K., Soppina, V., & Kanvah, S., *J. Photochem. Photobiol. B: Biol.*, 2020, *203*, 111732.
3. Y. Dubey, P. Mahalingavelar, D. Rajput, D. J. Shewale, V. Soppina and S. Kanvah, *Org. Biomol. Chem.*, 2023, **21**, 8393-8402.